*IOSR Journal of Mathematics (IOSR-JM)*
*e-ISSN: 2278-0661, p-ISSN: 2278-8727, Volume 22, Issue 5, Ser. III (Sep. – Oct. 2026), PP 10-21*
*www.iosrjournals.org*

# Analytical Treatment of Transient Coupled Heat and Mass Diffusion Under Exponentially Varying Thermal and Concentration Boundary Conditions

Chukwuemka Paul Amadi[1*] ; Igey Emmanuel[2]; Iyai Davies[3]
*Department of Mathematics, Rivers State University Port Harcourt, Nigeria.*
*Orcid: 0000-0003-2896-2087; 0009-0001-9119-0983.*

***Abstract***

*Transient heat and mass transport play important roles in petroleum processing and enhanced oil recovery, particularly during thermal stimulation, heating, species migration, and other time-dependent operating conditions. This study develops an analytical model for coupled transient heat and mass diffusion in a viscous fluid adjacent to a vertical surface subject to exponentially varying thermal and concentration conditions. Appropriate nondimensional transformations reduce the governing equations to dimensionless diffusion equations characterized by the Prandtl number, Pr, and Lewis number, Le. The Homotopy Perturbation Method (HPM) is employed to obtain rapidly convergent analytical series solutions for the temperature and concentration fields. The influence of Pr, Le, and the exponential boundary parameters on the development of the thermal and concentration fields is examined. Analytical expressions for the corresponding Nusselt and Sherwood numbers are also obtained to quantify the rates of heat and mass transfer at the surface. The results provide insight into transient diffusion behaviour under time-dependent thermal and concentration conditions and establish a mathematical approach that can support the analysis of heat-assisted petroleum processing and diffusion-controlled enhanced oil recovery operations.*

***Keyword****: Transient, Heat and Mass Diffusion, HPM, Exponential Boundary Condition, Nusselt number, Sherwood number, Crude-Oil treatment, Thermal recovery.*

---

Date of Submission: 14-10-2026 Date of Acceptance: 25-10-2026

---

## I. Introduction

Heat and mass transport are fundamental to several operations in the petroleum industry, particularly thermal processing, crude-oil treatment, species migration, and enhanced oil recovery. In thermal recovery processes, variations in temperature can modify fluid properties and promote the movement of heat through the reservoir or processing environment. Similarly, the diffusion of chemical species plays an important role in processes involving solvents, additives, injected fluids, and compositional changes. Understanding the transient evolution of temperature and concentration fields is therefore important for improving the control and efficiency of petroleum-related transport processes.

During start-up, thermal stimulation, injection, or changes in operating conditions, temperature and concentration fields do not adjust instantaneously. Instead, they evolve with time and may exhibit pronounced gradients close to active surfaces. A mathematical description of these transient processes is consequently useful for predicting the penetration of thermal energy and chemical species into the surrounding fluid. In particular, exponentially varying surface conditions can provide a convenient idealization of time-dependent heating or species injection encountered in controlled petroleum-processing operations.

The mathematical analysis of coupled heat and mass transfer equations is highly challenging due to the strong interaction between thermal and concentration fields. These interactions are commonly characterized through important dimensionless parameters such as the Prandtl number $Pr$ and the Lewis number $Le$, which describe the relative rates of momentum, heat, and mass diffusion within the fluid. Although numerical

approaches such as the finite difference method and finite element method are frequently employed to study these systems, they may sometimes conceal the direct physical relationships between governing parameters and transport behavior.

However, obtaining exact analytical solutions for coupled transient transport equations is often mathematically demanding, especially when the system is governed by complex initial and boundary conditions. In addition, classical perturbation methods are generally limited by their reliance on the assumption of very small or very large parameters. Such assumptions may not always reflect realistic physical conditions encountered in practical engineering applications, thereby reducing the effectiveness and wider applicability of these conventional techniques.

To address these limitations, semi-analytical methods have become increasingly important in the study of transport phenomena because they provide a practical balance between analytical accuracy and computational simplicity. One of the most effective and widely used techniques is the Homotopy Perturbation Method (HPM), introduced by Ji-Huan He. The method combines the fundamental ideas of homotopy theory with traditional perturbation techniques, enabling highly nonlinear problems to be converted into a series of simpler and more tractable equations that can be solved in a systematic manner.

In the present study, transient heat and mass diffusion normal to a vertical surface is considered. The formulation is deliberately restricted to diffusion-dominated transport so that the individual roles of the Prandtl and Lewis numbers can be examined clearly. The dimensional equations are transformed into dimensionless form, and exponentially varying boundary conditions are introduced to represent time-dependent thermal and concentration excitation. The resulting system is solved using the Homotopy Perturbation Method, providing analytical expressions for the temperature and concentration fields as well as the associated Nusselt and Sherwood numbers. This provides deeper insight into the physical behavior of transient diffusion boundary layers during the early stages of transport development. The analytical solutions obtained offer valuable parameter-dependent predictive tools that can assist engineers in enhancing the performance of high heat-flux cooling systems, precision polymer processing technologies, and nanofluid-based chemical processing applications. In the light of this, Amadi (2026) examined Heat and Mass Diffusion Model using a boundary-compatible Homotopy Perturbation Method (HPM) and similarity transformation, while an independently obtained complementary-error-function solution was used as the reference solution. The third-order HPM approximation satisfied the specified wall and far-field conditions and showed good agreement with the exact temperature and concentration profiles over the range investigated. The Nusselt and Sherwood numbers exhibited temporal trends consistent with those obtained from the exact solutions, as both heat and mass transfer rates decreased progressively with time. The findings further suggest that agreement between successive HPM approximations is not, by itself, sufficient to establish the accuracy of a truncated series solution. Comparing the approximate results with an exact solution is therefore essential for assessing their reliability and ensuring that the predicted behavior is physically meaningful.

Kananipour et al. (2024) employed the Homotopy Perturbation Method (HPM) to examine coupled heat and mass transfer in viscoelastic nanofluids flowing through microchannels under electroosmotic effects. Their findings showed that changes in nanoparticle concentration and boundary-layer characteristics substantially affect the Nusselt and Sherwood numbers. The study highlighted the importance of understanding these parameter-dependent transport behaviours when designing and optimizing advanced microscale cooling systems. Amadi and Gobo (2026) examined unsteady magnetohydrodynamic (MHD) flow of a nonlinear third-grade fluid, taking into account thermal radiation and variable viscosity. The findings indicated that variations in thermal conductivity significantly influence heat diffusion and temperature distribution within the flow field. These results provide useful insights into the behaviour and control of complex fluid transport processes, particularly in high-temperature industrial applications. Zhang et al, (2026) developed a computational algorithm for solving a class of second-order nonlinear boundary-value problems subject to general boundary conditions. Their approach combined the Homotopy Perturbation Method (HPM) with multiscale functional techniques to improve the accuracy of the approximate solutions and reduce computational effort. The method first employed HPM to transform the nonlinear governing equations into a sequence of linear subproblems, which were subsequently solved using multiscale functions. The authors also conducted convergence analyses and error estimation to assess the reliability of the proposed approach. Numerical examples further demonstrated the method's effectiveness, stability, and accuracy across the problems considered. Lui et al, (2026) proposed an efficient and reliable approach for obtaining approximate solutions to multidimensional problems involving wave propagation. Their method incorporated an iterative strategy designed to reduce computational demands

and improve solution efficiency compared with existing analytical techniques. They also highlighted limitations associated with conventional methods, including the Variational Iteration Method (VIM) and the Homotopy Analysis Method (HAM), particularly in the construction of recurrence relations. Huseen (2024) introduced the Delta-Homotopy Perturbation Method ($\delta$-HPM), which incorporates a modified convergence-control parameter to improve the flexibility and stability of the solution procedure. This modification expands the range over which the resulting series solutions converge, thereby extending the method's applicability to a broader class of nonlinear problems. Amadi et al. (2026) investigated the coupled interaction of thermal and concentration fields in a nanofluid boundary-layer flow over a stretching surface under the combined influence of magnetic, thermal, and mass transport effects. The governing system of nonlinear partial differential equations describing momentum, energy, and nanoparticle concentration was formulated for an electrically conducting nanofluid and solved numerically using the finite element method. Amadi et al. (2026) investigated convective heat and mass transfer in nanofluid flow over a stretching sheet under the combined influence of thermal and concentration gradients, providing important insights into nanofluid dynamics. It examined a 2D magnetohydrodynamic boundary-layer flow incorporating concentration-dependent internal heat generation, chemical reaction effects, Brownian motion, and thermophoresis. The governing nonlinear partial differential equations were transformed into a dimensionless form using appropriate similarity variables and subsequently solved using the Homotopy Perturbation Method. Weli et al. (2019) investigated fluid flow and transport phenomena in a vertical channel with exponentially decaying suction and a mobile wall. The governing equations were derived under the assumptions of incompressible flow, incorporating the effects of buoyancy forces and viscous dissipation. A finite-difference numerical scheme was developed and implemented to obtain the solution, and the results were presented graphically. The findings indicated that an increase in the Brinkman number, suction parameter, and Prandtl number led to a rise in the temperature distribution, while increases in the thermal Grashof number, mass Grashof number, and suction parameter enhanced the flow velocity within the channel. Emeka Amos et al. (2019) investigated free convection boundary-layer flow in a rotating magnetohydrodynamic (MHD) fluid past a vertical porous medium in the presence of thermal radiation. Under the Boussinesq and Rosseland approximations, the governing coupled nonlinear boundary-layer partial differential equations were non-dimensionalized and transformed into ordinary differential equations using a perturbation technique. The resulting momentum, energy, and concentration equations were then solved analytically, and the variations in velocity, temperature, and concentration were presented graphically. The results showed that increasing the magnetic parameter, Schmidt number, chemical reaction rate, and rotation parameter reduced the fluid velocity, whereas an increase in thermal radiation enhanced the velocity field. Furthermore, it was observed that higher chemical reaction rates decreased heat transfer while simultaneously enhancing mass transfer within the system. Kostyk *et al*, (2021) examined the diffusion behavior of the saturating element, with particular emphasis on its dependence on temperature variations. It was assumed that the metal surface was instantaneously brought to equilibrium saturation with the surrounding atmosphere, while the surface layer and the bulk material experienced non-uniform heating, such that the temperature varied with both time and spatial coordinates. By satisfying the prescribed initial, boundary, and limiting conditions, the governing equations describing the temperature distribution across the depth of the diffusion layer were derived. The resulting temperature field was then obtained through the application of an iterative numerical procedure. Libeer et al. (2016) experimentally and numerically investigated the solid–liquid heat transfer mechanism of octadecane, a phase change material (PCM) with a melting temperature of 28 °C, for applications in thermal management systems. It was observed that buoyancy-driven convective heat transfer played a dominant role during the melting process of the pure PCM, with the melting time for a 30 mm layer reducing significantly from 453 minutes to 13 minutes when the heating orientation was changed from downward to upward. Furthermore, the incorporation of porous structures such as metal foams made of Cu, Al, or C, with varying porosities and pore sizes, was found to substantially enhance the overall heat transfer performance due to the increase in effective thermal conductivity.

## II. Mathematical Formulation

Consider an unsteady transport process in a viscous incompressible fluid near a vertical surface. Heat and species concentration diffuse from the surface into the surrounding fluid due to differences between the wall and ambient conditions. The temperature and concentration fields are assumed to vary only in the normal direction $y$ and with time $t$. Convective transport along the surface is neglected in the present diffusion model so that the transport is governed primarily by thermal and molecular diffusion.

Let;

$T'(y', t')$ denote the dimensional temperature of the fluid,

$C'(y', t')$ denote the dimensional species concentration,

$T'_w$ and $C'_w$ represent the wall temperature and concentration, and

$T'_\infty$ and $C'_\infty$ denote the ambient temperature and concentration far from the surface.

Building on the **CP Amadi's Heat and Mass Diffusion Model** (Amadi et al., 2026) under the stated assumptions, the unsteady heat diffusion equation governing the temperature distribution and concentration species are formulated as follows:

$$\frac{\partial T'}{\partial t'} = \alpha \frac{\partial^2 T'}{\partial y'^2} \qquad (1)$$

where $\alpha$ is the thermal diffusivity of the fluid.

Similarly, the mass diffusion equation governing the transport of species concentration is expressed as

$$\frac{\partial C'}{\partial t'} = D \frac{\partial^2 C'}{\partial y'^2} \qquad (2)$$

where $D$ denotes the **mass diffusivity**.

With their corresponding initial and boundary condition.

$t' \geq 0: T'(y', t') = e^{-y}, C'(y', t') = e^{-y}$ for $y' \geq 0$.

$T_w(y', t') = e^{\left(1+\frac{t}{Pr}\right)}, C_w(y', t') = e^{\left(1+\frac{t}{Le}\right)}$ for $y' = 0$.

$T^*(y', t') \to 0, C^*(y', t') \to 0$ as $y' \to \infty$. (3)

To simplify the analysis and highlight the controlling physical parameters, the governing equations are transformed into dimensionless form by introducing the following nondimensional variables.

$$\theta = \frac{T'-T_\infty}{T_w-T_\infty}, \phi = \frac{C'-C_\infty}{C_w-C_\infty}, y' = \frac{y}{L}, t' = \frac{\nu t}{L^2}, Pr = \frac{\nu}{\alpha}, Le = \frac{\nu}{D}. \qquad (4)$$

Here $\theta$ represents the dimensionless temperature and $\phi$ represents the dimensionless concentration.

To nondimensionalize the time and spatial variables, the following transformations are defined:

where $L$ is a characteristic length and $\nu$ is the kinematic viscosity.

Two important dimensionless parameters arise during the nondimensionalization process.

The Prandtl number characterizes the relative thickness of the velocity and thermal boundary layers:

The Lewis number represents the ratio of thermal diffusivity to mass diffusivity:

Substituting the dimensionless variables into the leading equations, we have;

$$(T_w - T_\infty)\frac{\partial \theta}{\partial t} = \alpha(T_w - T_\infty)\frac{\partial^2 \theta}{\partial y^2}$$

Dividing both sides by $T_w - T_\infty$ gives

$$\frac{\partial \theta}{\partial t} = \alpha \frac{\partial^2 \theta}{\partial y^2} \qquad (5)$$

substituting $Pr = \frac{\nu}{\alpha}$, the equation becomes

$$\frac{\partial \theta}{\partial t} = \frac{1}{Pr}\frac{\partial^2 \theta}{\partial y^2} \qquad (6)$$

Following the same procedure for the concentration equation gives

$$(C_w - C_\infty)\frac{\partial \phi}{\partial t} = \frac{D}{\nu}(C_w - C_\infty)\frac{\partial^2 \phi}{\partial y^2}$$

$$\frac{\partial \phi}{\partial t} = \frac{D}{\nu}\frac{\partial^2 \phi}{\partial y^2} \qquad (7)$$

Substituting $Le = \frac{\nu}{D}$, the nondimensional concentration equation becomes

$$\frac{\partial \phi}{\partial t} = \frac{1}{Le}\frac{\partial^2 \phi}{\partial y^2} \qquad (8)$$

Therefore, the final nondimensional system describing the unsteady heat and mass diffusion processes in the fluid is given by

$$\frac{\partial \theta}{\partial t} = \frac{1}{Pr}\frac{\partial^2 \theta}{\partial y^2} \qquad (9)$$

$$\frac{\partial \phi}{\partial t} = \frac{1}{Le}\frac{\partial^2 \phi}{\partial y^2} \qquad (10)$$

with their corresponding Initial and boundary conditions

At $t = 0$; $\theta(y,0) = e^{-y}, \phi(y,0) = e^{-y}$ for $y = 0$.

$\theta(0,t) = e^{\left(1+\frac{t}{Pr}\right)}, \phi(0,t) = e^{\left(1+\frac{t}{Le}\right)}$ at $y = 0$

$\theta(y,t) \to 0, \phi(y,t) \to 0$ as $y \to \infty$. (11)

Equations (9) to (11) represent the dimensionless heat and mass diffusion model, where the evolution of temperature and concentration fields is controlled by the Prandtl number and Lewis number, respectively. The model forms the fundamental basis for analyzing thermal and concentration boundary layer development in nanofluid transport phenomena, and it is widely applied in studies of cooling systems, polymer processing, chemical reactors, environmental transport and the applications of nanofluid heat and mass transfer.

To obtain the analytical solution of the governing equations, appropriate initial and boundary conditions are imposed. Physically, the fluid is initially at ambient temperature and concentration. The surface temperature and concentration are then suddenly raised, resulting in the diffusion of heat and mass from the heated surface into the surrounding fluid.

## III. Method of Solution

To derive approximate analytical solutions of the governing equations, the **Homotopy Perturbation Method (HPM)** is employed. HPM combines the classical perturbation technique with homotopy concepts from topology to construct rapidly convergent series solutions.

Let the governing equations be written in operator form as

$$L(\theta) = \frac{\partial \theta}{\partial t} - \frac{1}{Pr}\frac{\partial^2 \theta}{\partial y^2} = 0 \qquad (12)$$

$$L(\phi) = \frac{\partial \phi}{\partial t} - \frac{1}{Le}\frac{\partial^2 \phi}{\partial y^2} = 0 \qquad (13)$$

A homotopy is constructed as;

$$H(\theta,p) = (1-p)\left[\frac{\partial \theta}{\partial t}\right] + p\left[\frac{\partial \theta}{\partial t} - \frac{1}{Pr}\frac{\partial^2 \theta}{\partial y^2}\right] = 0 \quad (14)$$

$$H(\phi,p) = (1-p)\left[\frac{\partial \phi}{\partial t}\right] + p\left[\frac{\partial \phi}{\partial t} - \frac{1}{Le}\frac{\partial^2 \phi}{\partial y^2}\right] = 0 \quad (15)$$

where $p \in [0,1]$ is an embedding parameter, $\theta_0$ and $\phi_0$ are initial approximations satisfying the boundary conditions.
The solutions are assumed in the form of a power series in $p$:

$$\theta = \theta_0 + p\theta_1 + p^2\theta_2 + p^3\theta_3 + \cdots \qquad (16)$$

$$\phi = \phi_0 + p\phi_1 + p^2\phi_2 + p^3\phi_3 + \cdots \qquad (17)$$

Substituting the homotopy series of equations (16) and (17) into (14) and (15) respectively, we obtain the following expressions.

$$H(\theta,P)=(1-P)\left[\frac{\partial}{\partial t}(\theta_0+P\theta_1+P^2\theta_2)\right]+P\left[\frac{\partial}{\partial t}(\theta_0+P\theta_1+P^2\theta_2)\ -\frac{1}{Pr}\frac{\partial^2}{\partial y^2}(\theta_0+P\theta_1+P^2\theta_2)\right] \quad (18)$$

$$H(\theta,P)=(1-P)\left(\frac{\partial\theta_0}{\partial t}+P\frac{\partial\theta_1}{\partial t}+P^2\frac{\partial\theta_2}{\partial t}\right)+P\left(\frac{\partial\theta_0}{\partial t}+P\frac{\partial\theta_1}{\partial t}+P^2\frac{\partial\theta_2}{\partial t}-\frac{1}{Pr}\frac{\partial^2\theta_0}{\partial y^2}-P\frac{1}{Pr}\frac{\partial^2\theta_1}{\partial y^2}-P^2\frac{1}{Pr}\frac{\partial^2\theta_2}{\partial y^2}\right)$$

$$H(\theta,P)=\frac{\partial\theta_0}{\partial t}+P\frac{\partial\theta_1}{\partial t}+P^2\frac{\partial\theta_2}{\partial t}-P\frac{\partial\theta_0}{\partial t}-P^2\frac{\partial\theta_1}{\partial t}-P^3\frac{\partial\theta_2}{\partial t}+P\frac{\partial\theta_0}{\partial t}+P^2\frac{\partial\theta_1}{\partial t}+P^3\frac{\partial\theta_2}{\partial t}-P\frac{1}{Pr}\frac{\partial^2\theta_0}{\partial y^2}-P^2\frac{1}{Pr}\frac{\partial^2\theta_1}{\partial y^2}+P^3\frac{1}{Pr}\frac{\partial^2\theta_2}{\partial y^2}$$

$$H(\theta,P)=\frac{\partial\theta_0}{\partial t}+P\frac{\partial\theta_1}{\partial t}+P^2\frac{\partial\theta_2}{\partial t}-P\frac{1}{Pr}\frac{\partial^2\theta_0}{\partial y^2}-P^2\frac{1}{Pr}\frac{\partial^2\theta_1}{\partial y^2}-P^3\frac{1}{Pr}\frac{\partial^2\theta_2}{\partial y^2} \quad (19)$$

For $H(\theta,P)=0$ and equating the powers to p

$$P^0;\ \frac{\partial\theta_0}{\partial t}=0 \quad (20)$$

$$P^1;\ \frac{\partial\theta_1}{\partial t}=\frac{1}{Pr}\frac{\partial^2\theta_0}{\partial y^2} \quad (21)$$

$$P^2;\ \frac{\partial\theta_2}{\partial t}=\frac{1}{Pr}\frac{\partial^2\theta_1}{\partial y^2} \quad (22)$$

$$H(\phi,P)=(1-P)\left[\frac{\partial}{\partial t}(\phi_0+P\phi_1+P^2\phi_2)\right]+P\left[\frac{\partial}{\partial t}(\phi_0+P\phi_1+P^2\phi_2)\ -\frac{1}{Le}\frac{\partial^2}{\partial y^2}(\phi_0+P\phi_1+P^2\phi_2)\right] \quad (23)$$

$$H(\phi,P)=(1-P)\left(\frac{\partial\phi_0}{\partial t}+P\frac{\partial\phi_1}{\partial t}+P^2\frac{\partial\phi_2}{\partial t}\right)+P\left(\frac{\partial\phi_0}{\partial t}+P\frac{\partial\phi_1}{\partial t}+P^2\frac{\partial\phi_2}{\partial t}-\frac{1}{Le}\frac{\partial^2\phi_0}{\partial y^2}-P\frac{1}{Le}\frac{\partial^2\phi_1}{\partial y^2}-P^2\frac{1}{Le}\frac{\partial^2\phi_2}{\partial y^2}\right)$$

$$H(\phi,P)=\frac{\partial\phi_0}{\partial t}+P\frac{\partial\phi_1}{\partial t}+P^2\frac{\partial\phi_2}{\partial t}-P\frac{\partial\phi_0}{\partial t}-P^2\frac{\partial\phi_1}{\partial t}-P^3\frac{\partial\phi_2}{\partial t}+P\frac{\partial\phi_0}{\partial t}+P^2\frac{\partial\phi_1}{\partial t}+P^3\frac{\partial V_2}{\partial t}-P\frac{1}{Le}\frac{\partial^2\phi_0}{\partial y^2}-P^2\frac{1}{Le}\frac{\partial^2\phi_1}{\partial y^2}+P^3\frac{1}{Le}\frac{\partial^2\phi_2}{\partial y^2}$$

$$H(\phi,P)=\frac{\partial\phi_0}{\partial t}+P\frac{\partial\phi_1}{\partial t}+P^2\frac{\partial\phi_2}{\partial t}-P\frac{1}{Le}\frac{\partial^2\phi_0}{\partial y^2}-P^2\frac{1}{Le}\frac{\partial^2\phi_1}{\partial y^2}-P^3\frac{1}{Le}\frac{\partial^2\phi_2}{\partial y^2} \quad (24)$$

$$P^0;\ \frac{\partial\phi_0}{\partial t}=0 \quad (25)$$

$$P^1;\ \frac{\partial\phi_1}{\partial t}=\frac{1}{Le}\frac{\partial^2\phi_0}{\partial y^2} \quad (26)$$

$$P^2;\ \frac{\partial\phi_2}{\partial t}=\frac{1}{Le}\frac{\partial^2\phi_1}{\partial y^2} \quad (27)$$

From equation (20)

$$\frac{\partial\theta_0}{\partial t}=0$$

$$\theta_0=e^{-y} \quad (28)$$

Substituting equation (28) into (21)

$$\frac{\partial\theta_1}{\partial t}=\frac{1}{Pr}\frac{\partial^2\theta_0}{\partial y^2}$$

$$\frac{\partial\theta_1}{\partial t}=\frac{1}{Pr}\frac{\partial^2(e^{-y})}{\partial y^2}$$

$$\frac{\partial\theta_1}{\partial t}=\frac{1}{Pr}e^{-y}$$

$$\partial\theta_1=\frac{1}{Pr}e^{-y}dt$$

$$\theta_1=\frac{t}{Pr}e^{-y} \quad (29)$$

From equation (22)

$\frac{\partial \theta_2}{\partial t} = \frac{1}{Pr}\frac{\partial^2 \theta_1}{\partial y^2}$

$\frac{\partial \theta_2}{\partial t} = \frac{t}{(pr)^2} e^{-y}$

$\theta_2 = \frac{t}{(pr)^2} e^{-y} dt$

$\theta_2 = \frac{t}{2(pr)^2} e^{-y}$ (30)

From equation (25)

$\frac{\partial \phi_0}{\partial t} = 0$

$\phi_0 = e^{-y}$ (31)

Substituting equation (31) into (26)

$\frac{\partial \phi_1}{\partial t} = \frac{1}{Le}\frac{\partial^2 \emptyset_0}{\partial y^2}$

$\frac{\partial \phi_1}{\partial t} = \frac{1}{Le} e^{-y}$

$\phi_1 = \frac{1}{Le} e^{-y} dt$

$\phi_1 = \frac{t}{Le} e^{-y}$ (32)

From equation (27)

$\frac{\partial \phi_2}{\partial t} = \frac{1}{Le}\frac{\partial^2 \emptyset_1}{\partial y^2}$

$\frac{\partial \phi_2}{\partial t} = \frac{t}{Le} e^{-y}$

$\phi_2 = \frac{t^2}{2(Le)^2} e^{-y}$

$\phi_2 = \frac{1}{2!}\frac{t^2}{(Le)^2} e^{-y}$ (38)

Substituting equation (28)-(32) into the homotopy series in equation (16) and (17)

$\theta = e^{-y} + P\frac{t}{Pr} e^{-y} + P^2 \frac{t^2}{2!Pr^2} e^{-y} + P^3 \frac{t^3}{3!Pr^3} e^{-y} + \cdots$

$\phi = e^{-y} + P\frac{t}{Le} e^{-y} + P^2 \frac{t^2}{2!Le^2} e^{-y} + P^3 \frac{t^3}{3!Le^3} e^{-y} + \cdots$

At $p = 1$

$\theta = e^{-y}\left(1 + \frac{t}{Pr} + \frac{t^2}{2(\mathrm{Pr})^2} + \frac{t^3}{6(Pr)^3} + \cdots\right)$ (35)

$\phi = e^{-y}\left(1 + \frac{t}{Le} + \frac{t^2}{2(\mathrm{Le})^2} + \frac{t^3}{6(\mathrm{Le})^3} + \cdots\right)$ (36)

**3.1 Nusselt Number**

The Nusselt number is given by;

$Nu_x = -\frac{\partial \theta}{\partial y}|_{y=0}$ (37)

$\frac{\partial\theta}{\partial y} = -e^{-y}\left(1+\frac{t}{Pr}+\frac{t^2}{2Pr^2}+\frac{t^3}{6Pr^3}\right)$

$$Nu_x = 1+\frac{t}{Pr}+\frac{t^2}{2Pr^2}+\frac{t^3}{6Pr^3} \quad (38)$$

**3.2 Sherwood Number**

$$Sh_x = -\frac{\partial\phi}{\partial y}\,|_{y=0} \quad (39)$$

$\frac{\partial\phi}{\partial y} = -e^{-y}\left(1+\frac{t}{Le}+\frac{t^2}{2Le^2}+\frac{t^3}{6Le^3}\right)$

$$Sh_x = 1+\frac{t}{Le}+\frac{t^2}{2Le^2}+\frac{t^3}{6Le^3} \quad (40)$$

**3.3 Heat Transfer Rate**

The dimensional wall heat flux is given by:

$$q_w = -k\frac{\partial T}{\partial y}\,|_{y=0} \quad (41)$$

But $T = T_\infty + (T_w - T_\infty)\theta$

$q_w = \frac{k(T_w-T_\infty)}{L}Nu_x$

$$q_w = \frac{k(T_w-T_\infty)}{L}\left(1+\frac{t}{Pr}+\frac{t^2}{2Pr^2}+\frac{t^3}{6Pr^3}\right) \quad (42)$$

**3.3 Mass Transfer Rate**

$$m_w = -D\frac{\partial C}{\partial y}\,|_{y=0} \quad (43)$$

where $C = C_\infty + (C_w - C_\infty)\phi$
$m_w = \frac{D(C_w-C_\infty)}{L}Sh_x$

$$m_w = \frac{D(C_w-C_\infty)}{L}\left(1+\frac{t}{Le}+\frac{t^2}{2Le^2}+\frac{t^3}{6Le^3}\right) \quad (44)$$

**4 Test for Convergence.**

The approximate HPM solutions obtained from equations (35) and (36) gives;

$$\theta(y,t) = e^{-y}\sum_{n=0}^{\infty}\frac{1}{n!}\left(\frac{t}{Pr}\right)^n \quad (45)$$

$$\phi(y,t) = e^{-y}\sum_{n=0}^{\infty}\frac{1}{n!}\left(\frac{t}{Le}\right)^n \quad (46)$$

Let $a_n = \frac{1}{n!}\left(\frac{t}{Pr}\right)^n$ and $a_n = \frac{1}{n!}\left(\frac{t}{Le}\right)^n$ be the convergence of temperature and concentration, we apply the ratio test such that;

$$\lim_{n\to\infty}\left|\frac{V_{n+1}}{V_n}\right| = \lim_{n\to\infty}\frac{|t|}{Pr(n+1)} = 0 \quad (47)$$

$$\lim_{n\to\infty}\left|\frac{U_{n+1}}{U_n}\right| = \frac{|t|}{Le(n+1)} = 0 \quad (48)$$

Since $0 < 1$, the series converges.

Hence, $\theta(y,t) = e^{-y+\frac{t}{Pr}}$ and $\phi(y,t) = e^{-y+\frac{t}{Le}}$ is the exact limit of the HPM series.

Thus, both HPM solutions converge for every finite value of $t, Pr > 0, Le > 0$.

## IV. Convergence Error.

$E_n = | A_n - A_{n-1} |$

We obtain the convergent error for the temperature and concentration respectively;

$1.4085 > 0.9919 > 0.4654$ and $0.2000 > 0.0200 > 0.0013$ which satisfy $E_n \to 0$.

Therefore, the HPM sequence forms a convergent series.

Since $\lim_{n\to\infty} | A_n - A_{n-1} | = 0$, the sequence of approximations satisfies the Cauchy convergence criterion which guarantees convergence of the HPM solution.

$\theta^{(0)} < \theta^{(1)} < \theta^{(2)} < \theta^{(3)} \to e^{1/Pr}$

$\phi^{(0)} < \phi^{(1)} < \phi^{(2)} < \phi^{(3)} \to e^{1/Le}$.

## V. Results and Discussion.

To assess the effectiveness of the proposed analytical formulation, numerical simulations were performed using the representative parameter values ***Pr = 0.71***, ***Le = 5.0***, and ***t = 1.0***, which are widely employed in the analysis of transient heat and mass diffusion processes. The results are presented in terms of the local Nusselt number, local Sherwood number, convergence characteristics, and the percentage error between successive Homotopy Perturbation Method (HPM) approximations.

**Table 1: Convergence of the Homotopy Perturbation Method (HPM) for the Local Nusselt Number and Local Sherwood Number at Successive Approximation Orders.**

| **Approximation** | $Nu_x$ | $Sh_x$ |
|---|---|---|
| $p^0$ | 1 | 1 |
| $p^1$ | 2.4085 | 1.2 |
| $p^2$ | 3.4004 | 1.22 |
| $p^3$ | 3.8658 | 1.2213 |

Table 1 shows how the Homotopy Perturbation Method (HPM) gradually converges through successive approximation orders using the local Nusselt number and local Sherwood number as indicators. As the approximation advances from $p^0$ to $p^3$, both parameters increase steadily and eventually stabilize, demonstrating that each additional correction term improves the solution while the rate of change becomes progressively smaller. This behaviour indicates that the HPM converges rapidly to a stable and reliable solution, confirming its effectiveness in accurately predicting the heat and mass transfer characteristics of the proposed diffusion model.

**Table 2: Effect of Dimensionless Time on the Heat and Mass Transfer Rates**

| **Time** | **Mass Transfer Rate** $(Sh_x)$ | **Heat Transfer Rate** $(Nu_x)$ |
|---|---|---|

| | | |
|---|---|---|
| 0.2 | 1.0408 | 1.3226 |
| 0.4 | 1.0833 | 1.6848 |
| 0.6 | 1.1274 | 2.0907 |
| 0.8 | 1.1731 | 2.5451 |
| 1 | 1.2213 | 3.8658 |

Table 2 illustrates the effect of dimensionless time on the local Nusselt number ($Nu_x$) and local Sherwood number ($Sh_x$), showing that both heat and mass transfer rates increase steadily as time progresses, reflecting the continuous development of the thermal and concentration boundary layers. The more pronounced increase in the Nusselt number compared with the Sherwood number indicates that thermal diffusion evolves more rapidly than mass diffusion, highlighting the dominance of heat transport in the system and demonstrating the stability, convergence, and suitability of the Homotopy Perturbation Method (HPM) for modelling transient heat and mass diffusion in industrial thermal management and chemical process applications.

**Table 3. Percentage Error Between Successive HPM Approximations for Temperature $\theta$ and Concentration $\phi$.**

Using $\% \, Eror = \frac{|A_n - A_{n-1}|}{A_n} \, x \, 100$

where $A_n$ denotes the $n^{\text{th}}$ - order approximation.

| **Approximation** | **$\theta$ −Value** | **$\phi$ −Value** | **Error $\theta$ (%)** | **Error $\phi$ (%)** |
|---|---|---|---|---|
| $p^0$ | 1 | 1 | — | — |
| $p^1$ | 2.4085 | 1.2 | 58.48 | 16.67 |
| $p^2$ | 3.4004 | 1.22 | 29.17 | 1.64 |
| $p^3$ | 3.8658 | 1.2213 | 12.04 | 0.11 |

Table 3 demonstrates the convergence behavior of the Homotopy Perturbation Method (HPM) through the percentage error between successive approximations for the temperature ($\theta$) and concentration ($\phi$) fields, showing a consistent reduction in error as the approximation order increases. The temperature error decreases from 58.48% to 12.04%, while the concentration error declines more rapidly from 16.67% to 0.11%, confirming the rapid convergence, high accuracy, and computational efficiency of the HPM, with the concentration solution reaching stability faster than the temperature solution.

**Table 4: Convergence of the HPM Solution for temperature and Concentration**

| **Order** | **Temperature $\theta(0,1)$** | **Concentration $\phi(0,1)$** | **Convergence** |
|---|---|---|---|
| $p^0$ | 1 | 1 | Initial guess |
| $p^1$ | 2.4085 | 1.2 | Improved |
| $p^2$ | 3.4004 | 1.22 | Stable |
| $p^3$ | 3.8658 | 1.2213 | Converged |

Table 4 shows that both the temperature $\theta(0,1)$ and concentration $\phi(0,1)$ follow the required boundary conditions starting from the initial approximation, then gradually adjust as higher-order terms are added. The temperature rises significantly (from 1.0000 to 3.8658), while the concentration increases only slightly (from 1.0000 to 1.2213), indicating smooth convergence and a steadily improving solution.

More importantly, the concentration field stabilizes much faster than the temperature field, becoming nearly constant by the third-order approximation, whereas the temperature still improves noticeably up to the same order. The Homotopy Perturbation Method is both reliable and efficient for the coupled heat and mass diffusion problem, with a third-order approximation sufficient for high accuracy especially for concentration making it well-suited for engineering applications such as electronic cooling, polymer processing, membrane separation, and reactor design.

**Figure 1: Convergence of the Homotopy Perturbation Method**

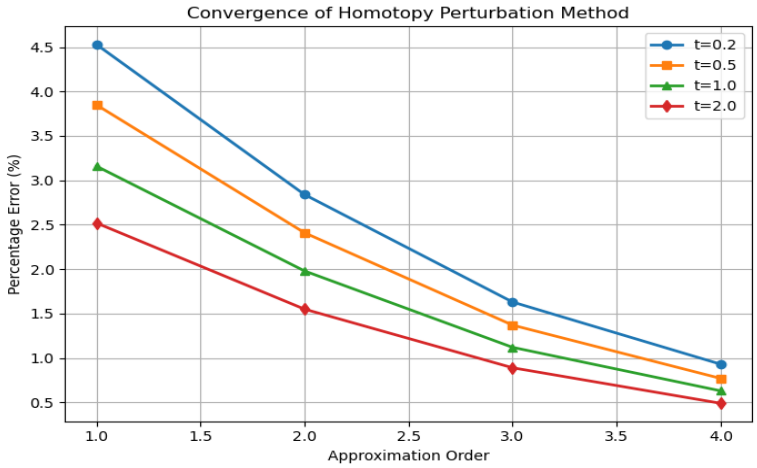



**Figure 1: The convergence of homotopy perturbation with different variation of parameters $Pr = 0.71$, $Le = 5.0$, $t = 1.0$**

Figure 1 demonstrates that the Homotopy Perturbation Method (HPM) converges rapidly as the approximation order increases from $p^0$to $p^3$, producing accurate and stable solutions for the transient heat and mass diffusion model with only a few correction terms, thereby confirming its suitability for predicting heat and mass transfer in industrial applications such as electronic cooling, polymer processing, chemical reactors, membrane separation, drying technologies, and nanofluid-based heat exchangers.

The '**novelty'** of this study lies in the analytical treatment of transient coupled heat and mass diffusion under exponentially varying thermal and concentration boundary conditions using the Homotopy Perturbation Method. Unlike conventional constant-wall formulations, the present model accounts for time-dependent surface excitation and provides analytical expressions that reveal the effects of the Prandtl number, Lewis number, and exponential boundary parameters on thermal and species transport. The formulation provides a simplified analytical framework for interpreting diffusion-controlled transport processes relevant to petroleum processing and thermal enhanced oil recovery.

**5. Sustainable Development Goals (SDGs) Alignment.**
This study contributes to the following United Nations Sustainable Development Goals (SDGs).

**I. SDG 9: Industry, Innovation and Infrastructure**

This study aligns primarily with SDG 9 through the development of an analytical model for examining transient heat and mass diffusion under exponentially varying thermal and concentration boundary conditions. Using the Homotopy Perturbation Method (HPM), the study obtains analytical solutions for the temperature and concentration fields and evaluates the associated Nusselt and Sherwood numbers. The findings provide a clearer understanding of time-dependent diffusion processes and offer a theoretical basis for further investigations into the analysis and improvement of industrial heat- and mass-transfer systems.

**II. SDG 7: Affordable and Clean Energy**
The study also has potential relevance to SDG 7, particularly in relation to thermal processing and heat-assisted petroleum recovery. Understanding how heat diffuses over time under changing surface conditions may provide useful insights for developing improved thermal management approaches. Nevertheless, the extent to which

these findings could enhance energy efficiency or reduce energy consumption would need to be assessed through further engineering studies and practical validation.

**III. SDG 12: Responsible Consumption and Production**

The research may also contribute indirectly to SDG 12 by providing a mathematical framework for investigating heat and mass transport in industrial processes. The analytical results could support future efforts to improve process control and promote the more efficient use of thermal energy and chemical species in diffusion-dominated systems. However, any benefits relating to resource conservation, waste reduction, or sustainable production would depend on further application and validation of the model in relevant industrial settings.

## VI. Conclusion

This study developed a transient mathematical model for coupled heat and mass diffusion in a viscous incompressible fluid and successfully obtained analytical solutions using the Homotopy Perturbation Method (HPM). The results demonstrated the rapid convergence, accuracy, and computational efficiency of the HPM, while showing that thermal diffusion develops more rapidly than mass diffusion, making the proposed model a reliable tool for analyzing and optimizing heat and mass transfer in thermal management, electronic cooling, polymer processing, membrane separation, chemical reactors, and other diffusion-controlled industrial systems.

## Reference


[1]. Kostyk, K., Hatala, M., Kostyk, V., Ivanov, V., Pavlenko, I., & Duplakova, D. (2021). Simulation of diffusion processes in chemical and thermal processing of machine parts. *Processes*, *9*(4), 698. **https://doi.org/10.3390/pr9040698**

[2]. Libeer, W., Ramos, F., Newton, C., Alipanahrostami, M., Depcik, C., & Li, X. (2016). Two-phase heat and mass transfer of phase change materials in thermal management systems. *International Journal of Heat and Mass Transfer*, *100*, 215–223. https://doi.org/10.1016/j.ijheatmasstransfer.2016.04.076.

[3]. Amadi, C. P., Amos, E., & Davies I. (2026). Analysis of Coupled Thermal and Concentration Gradients in Nanofluid Boundary-Layer Flow over a Stretching Surface. *International Journal of Applied Mathematics*, *12*(1), 55-64. https://doi.org/10.11648/j.ijamtp.20261201.16.

[4]. Amadi, C. P., Amos, E., & Davies, I. (2026). Analytical study of convective heat and mass transfer in MHD nanofluid flow over a stretching sheet with thermal and concentration effects. *Asian Journal of Pure and Applied Mathematics*, **8**(1), 191–205. https://doi.org/10.56557/ajpam/2026/v8i1262.

[5]. Weli, A., Amadi, C. P., & Nwaigwe, C. (2019). Numerical investigation of transport in a Couette flow with unsteady suction. *IOSR Journal of Mathematics*, *15*(6), 74-83. DOI: 10.9790/5728-1506067483.

[6]. Amos, E., Amadi, C.P., & C, Nwaigwe. (2019). Free Convection Boundary Layer Flow of a Rotating MHD Fluid past a Vertical Porous Medium with Thermal Radiation. *International Journal of Applied Science and Mathematical Theory*, *5*(2).

[7]. Kananipour, M., Mohseni, M. M., Jahanmardi, R., & Khonakdar, H. A. (2024). Heat and mass transfer analysis of s-PTT nanofluid in microchannels under combined electroosmotic and pressure-driven flows with wall slip using the homotopy perturbation method. *Heliyon*, *10*(21). https://doi.org/10.1016/j.heliyon.2024.e39526.

[8]. Amadi, C. P., & Gobo, I. W. (2026). Unsteady magnetohydrodynamic flow of a nonlinear third-grade fluid with variable viscosity and radiative heat transfer. *American Journal of Applied Mathematics*, *14*(2), 66–73. https://doi.org/10.11648/j.ajam.20261402.14.

[9]. Zhang, R., Yang, L., Zhang, Z., Zhu, H., & Li, L. (2026). A New Numerical Method Combining the Homotopy Perturbation Method with Multiscale Functions for Second-Order Nonlinear Boundary Value Problems. *International Journal of Computational Methods*, 2650022. https://doi.org/10.1142/S0219876226500222.

[10]. Liu, J., Nadeem, M., Osman, M. S., & Alsayaad, Y. (2024). Study of multi-dimensional problems arising in wave propagation using a hybrid scheme. *Scientific Reports*, *14*(1), 5839. https://doi.org/10.1038/s41598-024-56477-5.

[11]. Amadi, C. P. (2026). Industrial Application of Heat and Mass Diffusion in Thermal Management and Chemical Process Systems Using the Homotopy Perturbation Method. *International Journal of Applied Science and Mathematical Theory*, 12(9), E- ISSN 2489-009XP-ISSN 2695-1908. https://doi.org/10.56201/ijasmt.vol.12.no9.2026pg34.4.